



## Full Length Article

Growth of Cu<sub>2</sub>S thin films by atomic layer deposition using Cu(dmamb)<sub>2</sub> and H<sub>2</sub>S

Raphael Edem Agbenyeke<sup>a,b</sup>, Bo Keun Park<sup>a,b</sup>, Taek-Mo Chung<sup>a,b</sup>, Chang Gyoun Kim<sup>a,b,\*</sup>, Jeong Hwan Han<sup>a,c,\*</sup>

<sup>a</sup> Division of Advanced Materials, Korea Research Institute of Chemical Technology (KRICT), 141 Gajeong-Ro, Yuseong-Gu, Daejeon 34114, Republic of Korea

<sup>b</sup> Department of Chemical Convergence Materials, University of Science and Technology (UST), 217, Gajeong-Ro, Yuseong-Gu, Daejeon 34113, Republic of Korea

<sup>c</sup> Department of Materials Science and Engineering, Seoul National University of Science and Technology, Seoul 01811, Republic of Korea

## ARTICLE INFO

## Article history:

Received 27 March 2018

Revised 25 April 2018

Accepted 4 May 2018

Available online 5 May 2018

## Keywords:

Cu<sub>2</sub>S

Atomic layer deposition

bis(dimethylamino-2-methyl-2-butoxy)  
copper(II)

H<sub>2</sub>S

## ABSTRACT

In this study, atomic layer deposition (ALD) of Cu<sub>2</sub>S was explored using bis(dimethylamino-2-methyl-2-butoxy)copper(II) and 5% H<sub>2</sub>S combination as Cu and S sources, respectively. The reaction resulted in a high growth rate of ~0.22–0.24 nm/cycle at 150–200 °C owing to the high reactivity of the Cu precursor. At all investigated temperatures, Cu<sub>2</sub>S films with Cu oxidation state of +1 were obtained with negligible impurity levels. It was revealed that stoichiometric Cu<sub>2</sub>S films could be deposited at 120–150 °C, while sulfur deficient films was formed at 200 °C. Cu<sub>2</sub>S ALD process at low temperatures of 100–120 °C resulted in continuous film formation while the higher deposition temperatures of >150 °C led to island formation. Cu<sub>2</sub>S films showed p-type electrical characteristic with high hole concentrations of 4 × 10<sup>19</sup>–10<sup>21</sup> cm<sup>-3</sup> and Hall mobility of 2 cm<sup>2</sup>/vs. Lastly, the as-deposited Cu<sub>2</sub>S films exhibited an optical band gap of 1.2 eV which widened upon prolonged surface oxidation and in addition displayed NIR intra-band absorption.

© 2018 Published by Elsevier B.V.

## 1. Introduction

Cuprous sulfide series (Cu<sub>2-x</sub>S) including stoichiometric chalcocite (Cu<sub>2</sub>S), djurleite (Cu<sub>1.96</sub>S), digenite (Cu<sub>1.8</sub>S), and anilite (Cu<sub>1.76</sub>S) are an important class of Cu-based chalcogenides that have attracted significant research effort over the years due to their extensive application potential [1,2]. Apart from their earthly abundance and low cost, they exhibit phase dependent optical and electrical properties, which makes them promising for a variety of applications [2,3,4]. For instance, Cu<sub>2</sub>S is preferred as light absorber for photovoltaic applications due to its moderate charge carrier density and suitable band gap (~1.2 eV). It has also been pointed out as an excellent co-catalyst for CO<sub>2</sub> reduction [3]. On the other hand, non-stoichiometric phases such as Cu<sub>1.96</sub>S, Cu<sub>1.8</sub>S, and Cu<sub>1.76</sub>S possess high carrier densities due to the existing copper vacancies, which results in the formation of localized surface plasmon extinction bands in the near infra-red region and permits applications in bio-imaging and photothermal processes [5]. The

copper vacancies in non-stoichiometric copper sulfide also play an essential role in engineering new nanoheterostructure materials through cation exchange or alloying by acting as the diffusion pathway for the influx of guest ions and the out flux of Cu ions [6]. Various techniques have been employed for the synthesis of Cu<sub>2-x</sub>S thin films and nanoparticles including colloidal processes [6], sputtering [7], electrodeposition [8], successive ion layer deposition and reaction [9], aerosol-assisted chemical vapor deposition [10], pulsed chemical vapor deposition [11], chemical vapor deposition [11] and atomic layer deposition (ALD) [12–15]. ALD is the most preferred route for precise controls of film thickness and composition owing to the self-limiting nature of each ALD half reaction. It is also ideal for uniformly coating and decorating complex 3-dimensional materials. Due to the excellent quality and step coverage of copper sulfide films grown by ALD, its use has rapidly extended to many areas of study including catalysis, gas sensing and energy and environment applications. Copper sulfide thin film by ALD was firstly evaluated using a β-diketonate based Cu compound which forms strong bonding between metal and chelating ligand. Cu(thd)<sub>2</sub> (thd=2,2,6,6-tetramethyl-3,5-heptanedionate) with a combination of H<sub>2</sub>S at the deposition temperatures of 125–250 °C resulted in the formation of copper monosulfide (CuS) films at a low growth rate of 0.03 nm/cycle owing to poor

\* Corresponding authors at: Division of Advanced Materials, Korea Research Institute of Chemical Technology (KRICT), 141 Gajeong-Ro, Yuseong-Gu, Daejeon 34114, Republic of Korea.

E-mail addresses: [cgkim@kRICT.re.kr](mailto:cgkim@kRICT.re.kr) (C.G. Kim), [jhan@kRICT.re.kr](mailto:jhan@kRICT.re.kr) (J.H. Han).

reactivity of  $\text{Cu}(\text{thd})_2$  and/or steric hindrance effect caused by the bulky nature of Cu compound [16]. Another  $\beta$ -diketonate based Cu precursor  $\text{Cu}(\text{acac})_2$  was also examined with  $\text{H}_2\text{S}$  for  $\text{Cu}_{2-x}\text{S}$  ALD. This also yielded consistently low growth rate of 0.025 nm/cycle at 130–200 °C [12]. A different type of dimeric form Cu precursor, bis(N, N'-di-sec-butylacetamidinato)dicopper (I), was employed with  $\text{H}_2\text{S}$  reactant [13]. Although this process resulted in self-limiting  $\text{Cu}_2\text{S}$  ALD reaction with an improved growth rate of 0.09 nm/cycle at 90 °C, the higher growth rates of  $\text{Cu}_2\text{S}$  ALD are still necessary to make the process more attractive for light absorber layers and other applications that require relatively thick films.

Here, we report the ALD of  $\text{Cu}_2\text{S}$  films using a new precursor combination of bis(dimethylamino-2-methyl-2-butoxy)Cu(II) [ $\text{Cu}(\text{dmamb})_2$ ] and  $\text{H}_2\text{S}$ . The  $\text{Cu}(\text{dmamb})_2/\text{H}_2\text{S}$  chemistry yielded high  $\text{Cu}_2\text{S}$  film growth rate at 120–200 °C. Film composition, surface morphology, optical and electrical properties depending on the growth temperature were characterized with the aim of fine-tuning the film properties for future applications.

## 2. Experimental

The  $\text{Cu}_2\text{S}$  films were grown by ALD in a traveling wave type 4-inch chamber (Atomic-Class, CN-1) using  $\text{Cu}(\text{dmamb})_2$  (UP chemical,

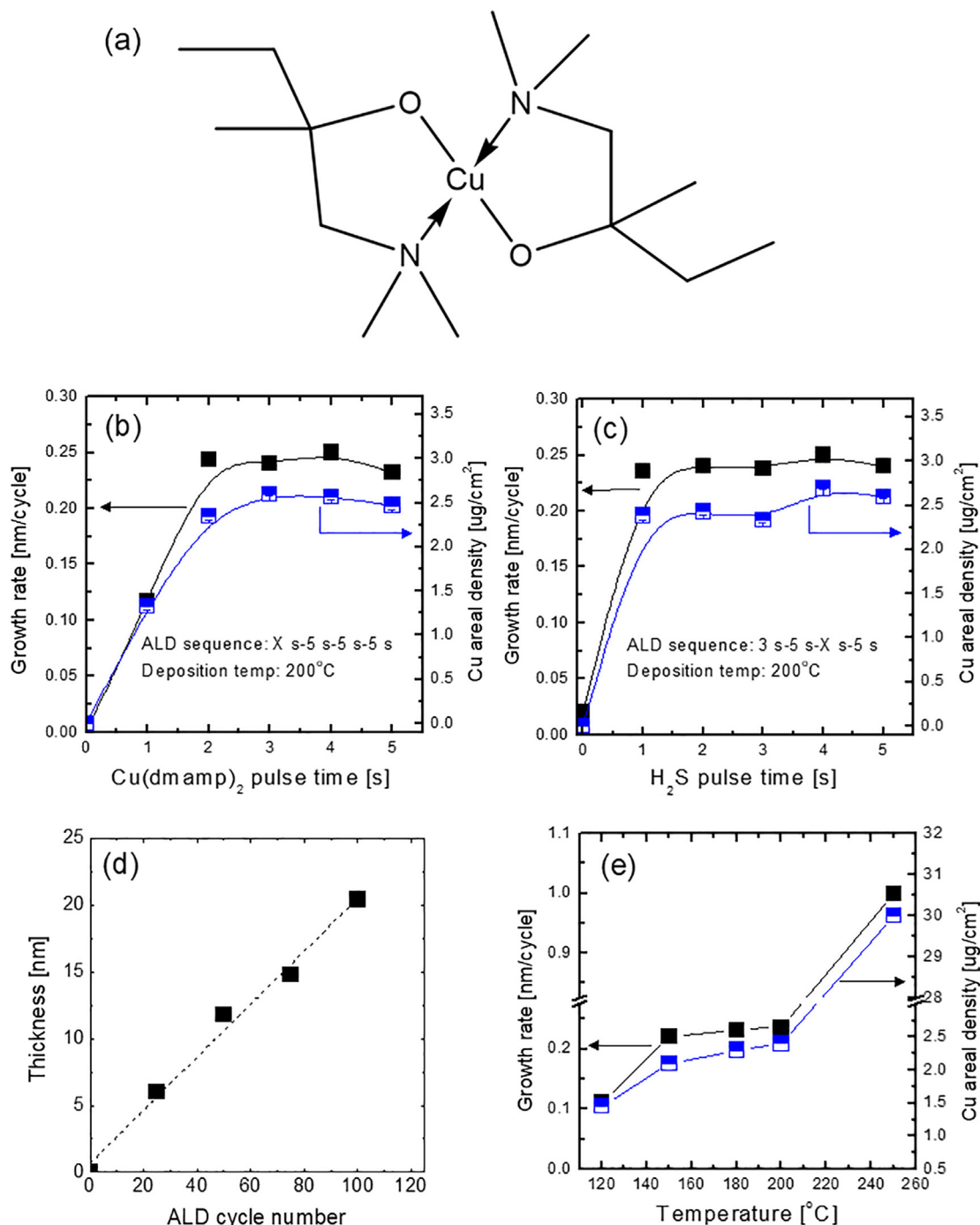


**Fig. 1.** (a) chemical structure of  $\text{Cu}(\text{dmamb})_2$  precursor. Changes in growth rate and areal density of  $\text{Cu}_2\text{S}$  films with varying (b)  $\text{Cu}(\text{dmamb})_2$  pulse time (c)  $\text{H}_2\text{S}$  pulse time. (d)  $\text{Cu}_2\text{S}$  film thickness as a function of ALD cycle number. (e) Temperature dependent growth rate and Cu areal density of  $\text{Cu}_2\text{S}$  films from 120 to 250 °C.

Korea) and a gas mixture of 95% N<sub>2</sub> and 5% H<sub>2</sub>S. The chemical structure of the Cu precursor consists of Cu–O covalent bonds and Cu–N coordinate bonds as shown in Fig. 1a. Cu(dmamb)<sub>2</sub> precursor is in liquid state at room temperature with high volatility of 0.9 Torr at 75 °C, whereas β-diketonate based Cu compounds of Cu(thd)<sub>2</sub> and Cu(acac)<sub>2</sub> are solid phase. The Cu precursor contained in a stainless steel bubbler type canister was heated at 60 °C and was delivered into the reaction chamber with the aid of ultrapure Ar gas at a flow rate of 50 sccm. The flow rate of H<sub>2</sub>S and Ar purge gases were 300 and 1000 sccm, respectively. The reaction was tested within a deposition temperature range of 100–250 °C. The films were grown on p-type Si (0 0 1) substrates and soda lime substrates for ex-situ characterization. Using alternating pulse steps of Cu(dmamb)<sub>2</sub> and H<sub>2</sub>S separated by Ar purge in the ALD sequence  $t_{\text{Cu}} s - 5 s - t_{\text{H}_2\text{S}} s - 5 s$ , (where  $t_{\text{Cu}}$  and  $t_{\text{H}_2\text{S}}$  represent precursor and reactant pulse times respectively), self-limiting growth conditions were optimized by varying Cu precursor and H<sub>2</sub>S dose time and Ar purge time. The changes in Cu areal density and growth rate of deposited films with different ALD pulse conditions were measured by spectroscopic ellipsometry (SE, Horiba Jobin Yvon UVISSEL) and X-ray fluorescence (XRF, ARLQUANTX, Thermo Fisher Scientific). Temperature dependent growth characteristics of Cu<sub>2</sub>S films were also examined using SE and XRF at the temperatures of 120–250 °C. High resolution X-ray diffraction (HRXRD, SmartLab, Rigaku) was used to identify the crystallinity and phase of the deposited films. X-ray photoelectron spectrometer (XPS, K-Alpha, Thermo Scientific) equipped with a monochromatic Al<sub>Kα</sub> X-ray source and Rutherford backscattering spectrometer (RBS, 6SDH-2 Pelletron Accelerator, NEC) were employed in examining the chemical binding state, stoichiometry, and purity of the films. Surface morphologies of the Cu<sub>2</sub>S films were observed using a field emission scanning electron microscope (FESEM, Hitachi S-4700) for the various deposition temperatures. The electrical and optical properties of the films were ascertained by Hall Effect measurement (HMS-5000, Ecopia) and UV–VIS–NIR spectroscopy (Shimadzu UV-2600) respectively.

### 3. Results and discussion

Fig. 1b and c depict the variation in growth rate and Cu areal density (which indicates the amount of Cu atoms loaded on the substrate surface per unit area) of Cu<sub>2</sub>S films with increasing Cu (dmamb)<sub>2</sub> pulse time at 200 °C. From the plots, a saturated growth rate of ~0.24 nm/cycle was obtained with Cu precursor and H<sub>2</sub>S pulse times of >2 s and >1 s, respectively. This is a rather impressive growth rate and to the best of our knowledge, the highest growth rate reported for Cu<sub>2</sub>S ALD. Owing to the facile surface reaction between the chemisorbed precursor molecules and the gaseous reactant, relatively short exposure times were required to achieve a self-limiting saturated growth. The significantly high growth rate and short process times are particularly desirable in terms of depositing thick films for photovoltaic absorbers and other applications. The high growth rate remained largely constant after a fourfold increase in the purge time from 5 to 20 s implying the efficient removal of unreacted precursor and reactant species and by-products (data not shown). Next, the changes in film thickness with cycle number were examined at 200 °C as shown in Fig. 1d. The growth rate was estimated from the slope of thickness vs. cycle number linear plot. Film thickness proportionally increased with ALD cycle number, and a steady state growth rate of ~0.20 nm/cycle was obtained. Fig. 1e displays the temperature dependent growth rate and Cu areal density of the Cu<sub>2</sub>S films deposited for 50 cycles. The growth rate increased with deposition temperature to 150 °C after which it exhibited a clear ALD temperature window up to 200 °C, where the growth rate of ~0.22–0.24 nm/cycle remained almost constant. Above 200 °C the growth rate

abruptly increased to ~1.0 nm/cycle with the simultaneous formation of pure Cu metal film instead of Cu<sub>2</sub>S. This can be explained by the thermal decomposition of the Cu precursor above 200 °C.

The crystal structure of ~50 nm-thick Cu<sub>2</sub>S films grown on silicon substrate at the deposition temperatures of 120–200 °C were investigated by high resolution XRD. As depicted in Fig. 2, irrespective of deposition temperature, strong diffraction peaks were observed at 26.6°, 37.2°, and 54.6° corresponding to (0 0 2), (1 0 2), and (0 0 4) planes of hexagonal structure Cu<sub>2</sub>S. This indicates the predominant formation of high chalcocite phase in the polycrystalline films. A relatively weak peak at 40.75° which is corresponding to the (2 2 5) plane of monoclinic low chalcocite was observed at 150 and 180 °C. At 200 °C the peak intensities slightly decreased, signifying the possible reduction of high and low chalcocite (Cu<sub>2</sub>S) phases at the higher temperature.

XPS analysis was used to examine the chemical binding state and composition of the Cu<sub>2</sub>S films as shown in Fig. 3. Prior to the measurements, the samples were sputtered with Ar<sup>+</sup> ion to eliminate surface contaminants. The adventitious C 1s peak at 284.5 eV was used as a reference to calibrate all other spectra. Fig. 3a depicts the Cu 2p high resolution XP spectra for Cu<sub>2</sub>S films deposited at different temperatures. Independent of deposition temperature the Cu 2p<sub>3/2</sub> peaks were symmetrically centered at 932.8 eV corresponding to a pure Cu<sup>+</sup> state, indicating Cu<sub>2</sub>S formation [9,10]. In addition, absence of shake up satellite peaks at 942.9 and 963.3 eV suggests successful deposition of pure Cu<sub>2</sub>S phase with a singular Cu<sup>+</sup> chemical state. Similarly, the S 2p<sub>3/2</sub> peaks in Fig. 3b were observed at 161.5 eV for all deposited films, lining up perfectly with reported values for sulfur in Cu<sub>2</sub>S. Fig. 3c shows the C and N 1s XP spectra for the films deposited at various temperatures after surface sputtering. Insignificant peaks were detected within all films, indicating the growth of highly pure Cu<sub>2</sub>S films. In the O 1s spectra depicted in Fig. 3d, two sub-peaks were identified, one at 530.4 eV corresponding to Cu–O bond and the other at 531.9 eV corresponding to Si–O bond originating from the silicon substrate. The peak at the lower binding energy disappeared after Ar<sup>+</sup> sputtering indicating pure Cu<sub>2</sub>S films at all temperature conditions while the peak at higher binding energy persisted due to the porosity of the Cu<sub>2</sub>S films which permitted detection of the underlying silicon substrate. To obtain accurate film stoichiometry, RBS analysis was used to measure the Cu/S ratio of the films. Fig. 4

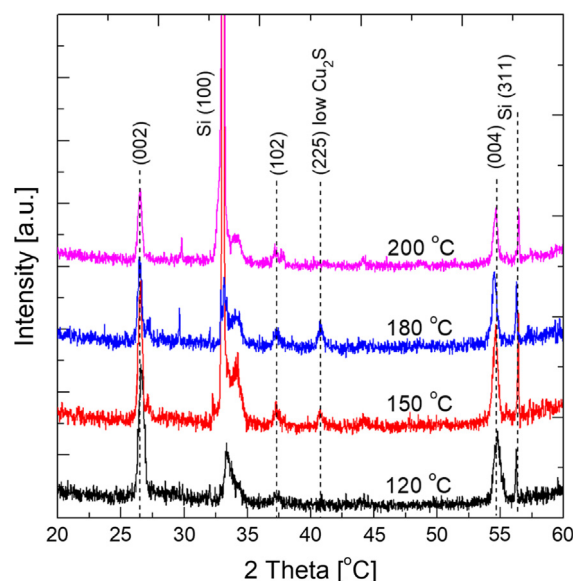


Fig. 2. High resolution XRD pattern of Cu<sub>2</sub>S films deposited at 120, 150, 180 and 200 °C.

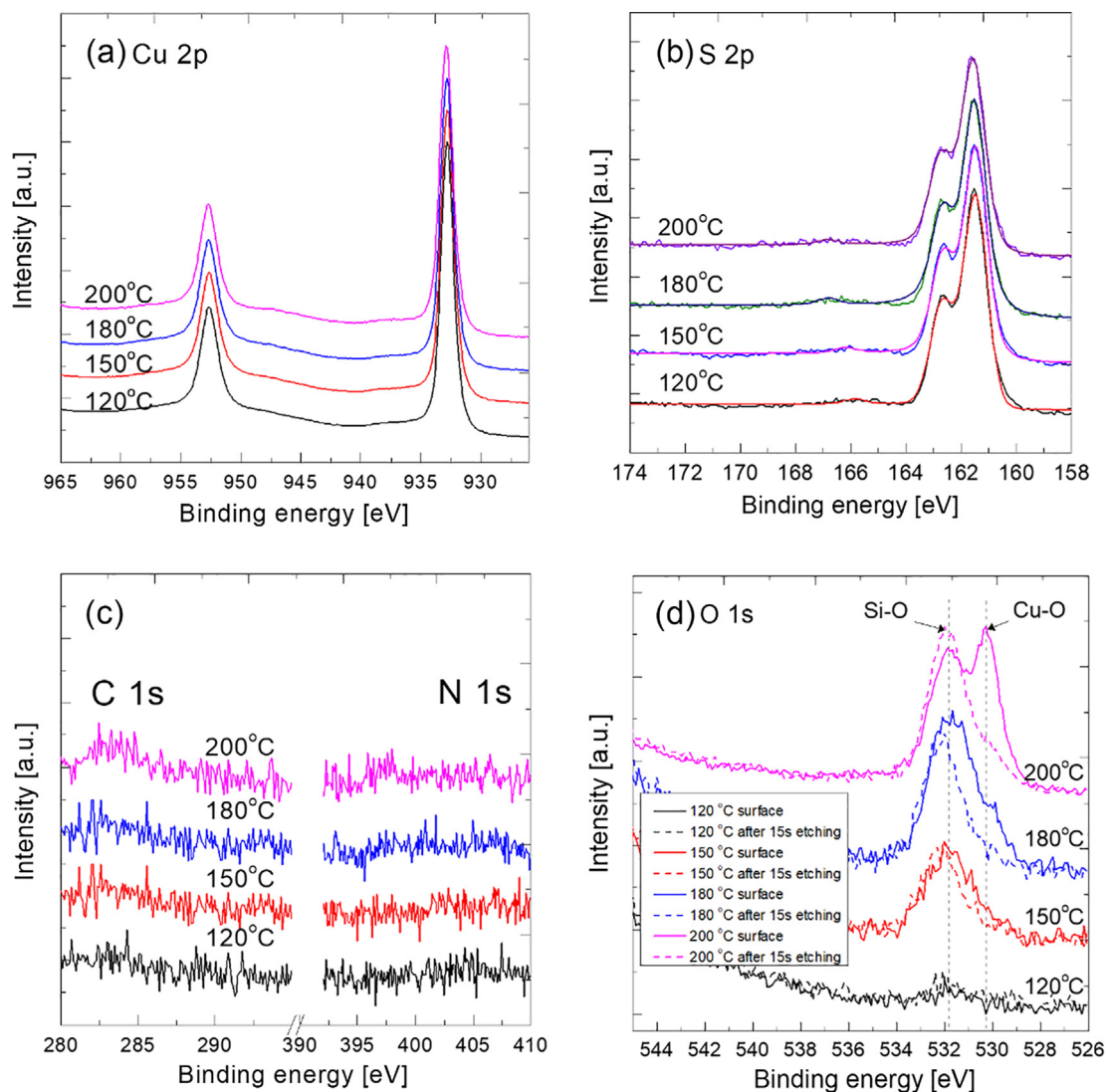


Fig. 3. XPS high resolution spectra of (a) Cu 2p, (b) S 2p, (c) C 1s and N 1s, and (d) O 1s for  $\text{Cu}_2\text{S}$  films grown at 120, 150, 180 and 200 °C.

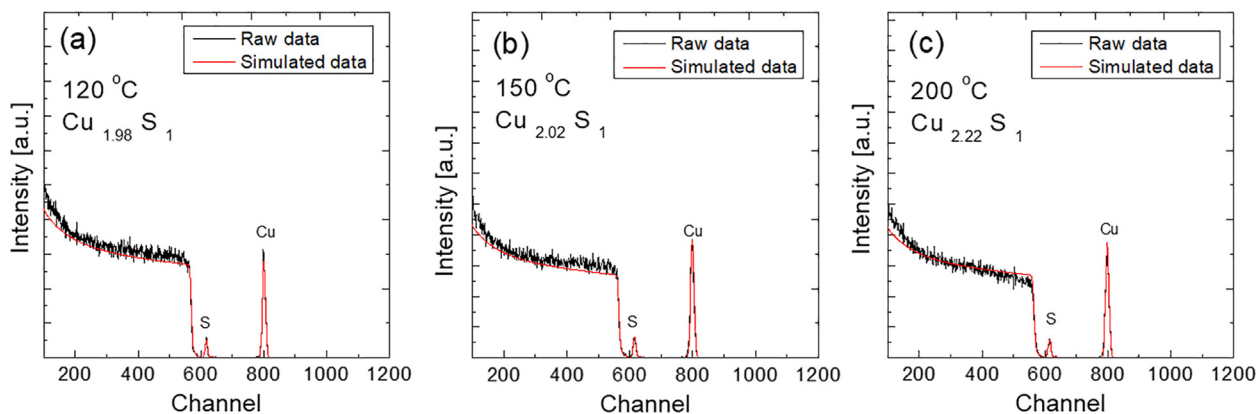


Fig. 4. RBS spectra of  $\sim 50$  nm thick  $\text{Cu}_2\text{S}$  films grown at (a) 120, (b) 150 and (c) 200 °C.

shows the RBS spectra of the films deposited at 120, 150, and 200 °C. The analysis revealed highly stoichiometric  $\text{Cu}_2\text{S}$  films at low deposition temperatures of 120 and 150 °C, respectively. On the other hand, sulfur deficient  $\text{Cu}_{2.02}\text{S}_{0.9}$  film was achieved at a higher deposition temperature of 200 °C. This might be due to evaporation of sulfur from the film.

The morphology of the films was investigated by field emission scanning electron microscopy (FESEM) as shown in Fig. 5. At relatively higher deposition temperatures of 150 and 200 °C, the films produced were highly discontinuous with clearly visible voids, whereas dense and continuous films were obtained at 100 and 120 °C. The formation of isolated domains gradually increased as

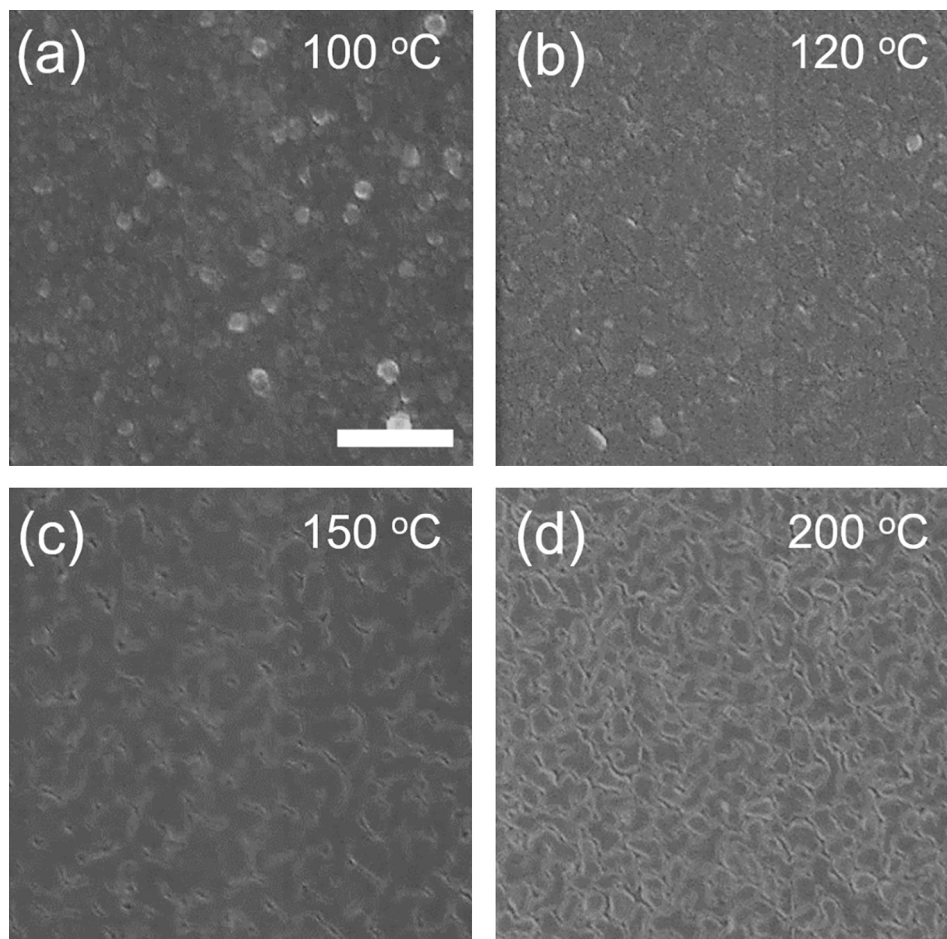


Fig. 5. FESEM images of  $\text{Cu}_2\text{S}$  films deposited on silicon substrates at (a) 100, (b) 120, (c) 150, and (d) 200 °C. (scale bar is 0.5  $\mu\text{m}$ ).

the growth temperature increased. This is a common phenomenon and can be attributed to the high mobility of Cu at elevated temperatures, which leads to preferential cohesion. At low temperatures, the films are less mobile on the substrate and hence form more uniform and continuous film.

Electrical properties of  $\sim 50$  nm thick films deposited on glass substrates at the various temperatures of 100–180 °C were examined by Hall measurement as displayed in Fig. 6. All films exhibited p-type characteristics with rather high carrier concentrations of

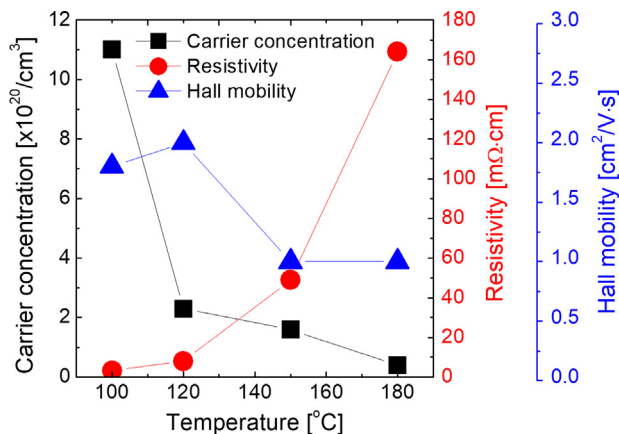


Fig. 6. Carrier concentration, resistivity, and Hall mobility of  $\text{Cu}_2\text{S}$  films grown at various deposition temperatures.

$4 \times 10^{19}$ – $10^{21} \text{ cm}^{-3}$ . As described in earlier reports, stoichiometric  $\text{Cu}_2\text{S}$  films generally exhibit moderate carrier concentrations in the order of  $10^{17}$ – $10^{18} \text{ cm}^{-3}$  [15,17]. Here, the high carrier concentrations of the deposited films can be ascribed to formation of surface  $\text{CuO}_x$  which concurrently generates significant Cu vacancy in the underlying  $\text{Cu}_2\text{S}$  film. Previous studies reported that rapid surface oxidation of  $\text{Cu}_2\text{S}$  upon exposure to ambient conditions results in a spike in the carrier concentration [14,15,17]. The carrier concentration steadily decreased with temperature and the resistivity values sharply increased from 100 to 180 °C due to the porous surface morphology of the films at higher temperatures. The film deposited at 200 °C was too resistive to obtain reliable data owing to the high discontinuity of the film. As high carrier mobility is a desirable characteristic for electronic and photovoltaic applications, Hall mobility of  $\text{Cu}_2\text{S}$  film was estimated by Hall measurement. The Hall mobility of the  $\text{Cu}_2\text{S}$  films showed the highest value of  $2 \text{ cm}^2/\text{Vs}$  for the film deposited at 120 °C, and decreased with increasing growth temperature which might be due to formation of many voids as observed by FESEM.

The response of the films to the electromagnetic spectrum was investigated by UV–VIS–NIR spectroscopy within a wavelength range of 300–1300 nm. As depicted in Fig. 7, the as-deposited film showed high transmittance of  $>90\%$  in the 1000–1300 nm wavelength region and a decrease in transmittance around 1000–1050 nm which corresponds to a band gap of  $\sim 1.2 \text{ eV}$  (solid line). Comparable spectra and optical band gap have been obtained for previously reported  $\text{Cu}_2\text{S}$  films [14,17,18]. The  $\text{Cu}_2\text{S}$  films were then kept in ambient conditions for about 3 months and measured

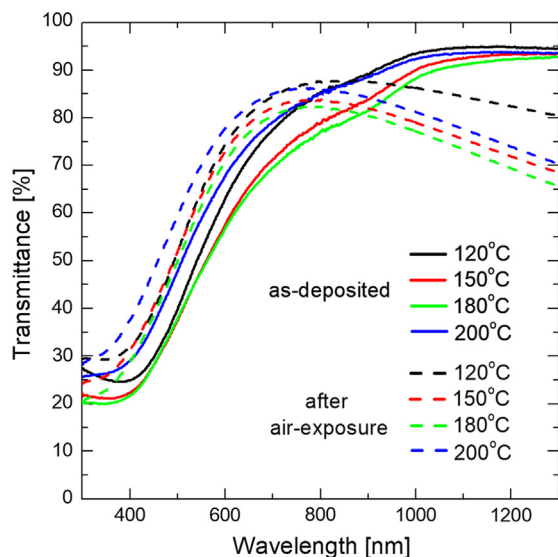


Fig. 7. Transmittance of  $\text{Cu}_2\text{S}$  films as-deposited (solid line) and after long exposure to ambient conditions (dashed line).

again to observe the effect of long air exposure times to the optical properties (dashed line). The transmittance in the NIR regime decreased for films exposed to ambient conditions in comparison to the as deposited state. This is due to further creation of Cu vacancies during surface oxidation which leads to free-carrier intra-band absorbance [2,5,17]. Besides the increase in absorption at long wavelengths, the spectra of the films blue shifted signifying a widening of the band gap. This can also be explained by the removal of electrons from the valence band edge during film oxidation which essentially widens the band gap, a phenomenon commonly referred to as the Moss-Burstein effect [2,11].

#### 4. Conclusion

In this report, we discussed the atomic layer deposition of  $\text{Cu}_2\text{S}$  films using a  $\text{Cu}(\text{dmamb})_2/\text{H}_2\text{S}$  chemistry. The process exhibited ALD temperature window of 150–200 °C, where a remarkably high growth rate of 0.22–0.24 nm/cycle was achieved. Above 200 °C pure copper metal films were deposited due to the thermal decomposition of Cu precursor. XPS and RBS analysis revealed that formation of stoichiometric  $\text{Cu}_2\text{S}$  films with negligible impurity levels at the temperatures of 120 and 150 °C.  $\text{Cu}_2\text{S}$  films deposited at low temperatures of 100–120 °C were densely arranged without voids while films grown at high temperatures of 150–200 °C were more prone to island formation.  $\text{Cu}_2\text{S}$  ALD films showed p-type property with high carrier concentration levels from  $4 \times 10^{19}$  to  $10^{21} \text{ cm}^{-3}$ . It was found that as-deposited  $\text{Cu}_2\text{S}$  films exhibited an optical band gap of 1.2 eV. After long air exposure, a widening of optical band and increased NIR intra-band absorption were observed. Finally we remark that  $\text{Cu}(\text{dmamb})_2/\text{H}_2\text{S}$  ALD process with highly improved growth rate and excellent film quality can be useful for various applications.

#### Author contributions

The manuscript was written through contributions of all authors. All authors have given approval to the final version of the manuscript.

#### Notes

The authors declare no competing financial interests.

#### Acknowledgment

This work was supported by Korea Research Institute of Chemical Technology (SI1803, Development of smart chemical materials for IoT device).

#### References

- [1] D. Zhang, A.B. Wong, Y. Yu, S. Brittman, J. Sun, A. Fu, B. Beberwyck, A.P. Alivisatos, P. Yang, Phase-Selective cation-exchange chemistry in sulfide nanowire systems, *J. Am. Chem. Soc.* 136 (2014) 17430–17433.
- [2] Y. Zhao, H. Pan, Y. Lou, X. Qiu, J.J. Zhu, C. Burda, Plasmonic  $\text{Cu}_{2-x}\text{S}$  nanocrystals: optical and structural properties of copper-deficient copper(I) sulfides, *J. Am. Chem. Soc.* 131 (2009) 4253–4261.
- [3] A. Manzi, T. Simon, C. Sonnleitner, M. Döblinger, R. Wyrwich, O. Stern, J.K. Stolarczyk, J. Feldmann, Light-induced cation exchange for copper sulfide based  $\text{CO}_2$  reduction, *J. Am. Chem. Soc.* 137 (2015) 14007–14010.
- [4] S.K. Han, M. Gong, H.B. Yao, Z.M. Wang, S.H. Yu, One-pot controlled synthesis of hexagonal-prismatic  $\text{Cu}_{1.94}\text{S}$ -ZnS,  $\text{Cu}_{1.94}\text{S}$ -ZnS- $\text{Cu}_{1.94}\text{S}$ ,  $\text{Cu}_{1.94}\text{S}$ -ZnS- $\text{Cu}_{1.94}\text{S}$ -ZnS- $\text{Cu}_{1.94}\text{S}$  heterostructures, *Angew. Chem. Int. Ed.* 51 (2012) 6365–6368.
- [5] I. Kriegel, C. Jiang, J. Rodríguez-Fernández, R.D. Schaller, D.V. Talapin, E. Como, J. Feldmann, Tuning the excitonic and plasmonic properties of copper chalcogenide nanocrystals, *J. Am. Chem. Soc.* 134 (2012) 1583–1590.
- [6] L.D. Trizio, L. Manna, Forging colloidal nanostructures via cation exchange reactions, *Chem. Rev.* 116 (2016) 10852–10887.
- [7] J.A. Thornton, W.W. Anderson, High performance all-sputter deposition  $\text{Cu}_2\text{S}/\text{CdS}$  junctions, *Appl. Phys. Lett.* 40 (1982) 622.
- [8] K. Anuar, Z. Zainal, M.Z. Hussein, N. Saravanan, I. Haslina, Cathodic electrodeposition of  $\text{Cu}_2\text{S}$  thin film for solar energy conversion, *Solar Energy Mater. Solar Cells* 73 (2002) 351–365.
- [9] F. Zhuge, X. Li, X. Gao, X. Gan, F. Zhou, Synthesis of stable amorphous  $\text{Cu}_2\text{S}$  thin films by successive ion layer adsorption and reaction method, *Mater. Lett.* 63 (2009) 652–654.
- [10] S. Schneider, J.R. Ireland, M.C. Hersam, T.J. Marks, Copper(I) *tert*-butylthiolato clusters as single-source precursors for high-quality chalcocite thin films: film growth and microstructure control, *Chem. Mater.* 19 (2007) 2780–2785.
- [11] I. Carbone, Q. Zhou, B. Vollbrecht, L. Yang, S. Medling, A. Bezryadina, F. Bridges, G.B. Alers, J.T. Norman, T. Kinmen, Pulsed chemical vapor deposition of  $\text{Cu}_2\text{S}$  into a porous  $\text{TiO}_2$  matrix, *J. Vac. Sci. Technol. A* 29 (2011), 051505(1–5).
- [12] N. Schneider, D. Lincot, F. Donsanti, Atomic layer deposition of copper sulfide thin films, *Thin Solid Films* 600 (2016) 103–108.
- [13] A.B.F. Martinson, Jeffrey W. Elam, M.J. Pellin, Atomic layer deposition of  $\text{Cu}_2\text{S}$  for future application in photovoltaics, *Appl. Phys. Lett.* 94 (2009), 123107(1–3).
- [14] S.C. Riha, R.D. Schaller, D.J. Gosztola, G.P. Wiederrecht, A.B.F. Martinson, Photoexcited carrier dynamics of  $\text{Cu}_2\text{S}$  thin films, *J. Phys. Chem. Lett.* 5 (2014) 4055–4061.
- [15] A.B.F. Martinson, S.C. Riha, E. Thimsen, J.W. Elam, M.J. Pellin, Structural, optical, and electronic stability of copper sulfide thin films grown by atomic layer deposition, *Energy Environ. Sci.* 6 (2013) 1868–1878.
- [16] J. Johansson, J. Kostamo, M. Karppinen, L. Niinisto, Growth of conductive copper sulfide thin films by atomic layer deposition, *J. Mater. Chem.* 12 (2002) 1022–1026.
- [17] S.C. Riha, S. Jin, S.V. Baryshev, E. Thimsen, G.P. Wiederrecht, A.B.F. Martinson, Stabilizing  $\text{Cu}_2\text{S}$  for photovoltaics one atomic layer at a time, *ACS Appl. Mater. Interfaces* 5 (2013) 10302–10309.
- [18] E. Thimsen, Q. Peng, A.B.F. Martinson, M.J. Pellin, J.W. Elam, Ion exchange in ultrathin films of  $\text{Cu}_2\text{S}$  and ZnS under atomic layer deposition conditions, *Chem. Mater.* 23 (2011) 4411–4413.